ELSEVIER

International Journal of Mass Spectrometry 203 (2000) 177–186

International Journal of Mass Spectrometry

Analysis of oxygen-18 in orthophosphate by electrospray ionisation mass spectrometry

Rebeca Alvarez[a], Louise A. Evans[a,*], Paul Milham[b], Michael A. Wilson[a]

[a]*Department of Chemistry, Materials and Forensic Science, University of Technology, Sydney, PO Box 123, Broadway, New South Wales 2007, Australia*

[b]*New South Wales Department of Agriculture, LMB21, Orange, New South Wales 2800, Australia*

Received 12 April 2000; accepted 4 August 2000

Abstract

Isotope distributions in phosphate are useful measurements in geochemical systems since they give information on origin and environmental oxygen exchange processes. It is often necessary to perform measurements rapidly at the parts per million level on milligram quantities of sample. However, current methodologies require conversion to gas and/or time consuming multiple precipitation steps or insensitive nuclear magnetic resonance (NMR) techniques. In the electrospray method developed here, lengthy analyses requiring precipitation of phosphate are unnecessary. Moreover, there is no requirement for conversion to a simple gas and indirect evaluation. Accuracy is demonstrated by good agreement with NMR measurements on concentrated laboratory prepared chemical solutions. After dilution, electrospray analyses gave similar results. (Int J Mass Spectrom 203 (2000) 177–186) © 2000 Elsevier Science B.V.

Keywords: Orthophosphate; Metaphosphate; Electrospray ionisation mass spectrometry (ESI-MS); Oxygen-18; Isotope

1. Introduction

Oxygen isotope ratios in phosphate have been widely used in geochemistry for paleoclimatological and paleoenvironmental studies as well as for studies involving tracers of phosphate transport and cycling in the environment [1–5]. These include studies of adsorption on clays, soil phosphate, and sedimentary apatites including variants with high phosphorus contents such as phosphorites [6–9]. Oxygen isotope ratios have also been used in the study of the formation of biominerals containing phosphorus such as apatite [10–13]. However application has been limited by the time needed to complete an analysis. Previous methods [7,14] have involved a lengthy analysis requiring precipitation of phosphate as the magnesium ammonium salt, $MgNH_4PO_4.6H_2O$, followed by mixing with pure carbon, heating at 500 °C to remove ammonia and water (leaving MgP_2O_7), and then transformation of the oxygen in phosphate to carbon monoxide by microwave reaction with carbon. The carbon monoxide is then analysed by emission spectroscopy by examining the different emission bands for $C^{18}O$, $C^{17}O$, and $C^{16}O$. More recently, other workers [15] used a method of analysis in which phosphate is precipitated as silver phosphate followed by thermal decomposition at 1000 °C to give oxygen.

* Corresponding author. E-mail: louise.evans@uts.edu.au

1387-3806/00/$20.00 © 2000 Elsevier Science B.V. All rights reserved
PII S1387-3806(00)00297-9

The recovered oxygen is then converted to carbon dioxide and the ^{18}O, ^{17}O, and ^{16}O carbon dioxide measured by isotope ratio mass spectrometry. Another time consuming mass spectrometric method involves a number of precipitation steps leading to precipitation as bismuth phosphate followed by oxygen release with bromine trifluoride [16] and measurement of oxygen directly.

Very recently Holmden and co-workers [17] presented a direct loading negative thermal ion mass spectrometric technique, which does not require the conversion of phosphate to carbon dioxide. However, it still requires relatively laborious pre-purification steps and tedious sample mounting procedures. This technique gives good sensitivity but is not amenable to rapid automated analyses of large numbers of samples. ^{31}P nuclear magnetic resonance (NMR) is a useful method of analysis of phosphate with different isotopic distributions because the differently isotopically substituted phosphorus nuclei resonate at different chemical shifts [18,19]. However NMR is notoriously insensitive and unsuitable at the ppm level and lower.

In principle, electrospray ionisation mass spectrometry (ESI-MS) [20,21] could be used to analyse phosphate directly and rapidly. There have been no previous estimations of isotope distributions in phosphate by ESI-MS. Hence in this article we explore ESI-MS as a tool for analysing phosphate. This technique works by transferring ions from solution phase to gas phase for detection but there are a number of possible difficulties in the method. Some are trivial, for example, phosphate can exist in equilibrium with its conjugate Bronsted acid and hence complications may occur if there are changes in concentrations as equilibrium is established. However this problem is easily overcome by buffering; others are more complex. Quantitative estimation of various isotopically substituted phosphates may not be a simple linear calibration of detector response versus concentration [22]. Moreover, different isotopically substituted species may charge differently. Further, singly charged ions are normally observed as their hydrated species, i.e. water ligands are present and charged ions may lose one or more ligands resulting in different responses. Finally, during this process it must be established that oxygen exchange does not occur to ligands otherwise isotope distribution information is lost.

2. Materials and methods

2.1. Synthesis of unlabeled and labeled potassium dihydrogen orthophosphate

Starting material, phosphorus oxychloride ($POCl_3$) (Ajax Chemicals), was purified by distillation under a dry nitrogen atmosphere. The glassware was flame-dried under a high vacuum and allowed to cool under a dry nitrogen atmosphere. The first and third fractions were collected at temperatures below and above the boiling point of phosphorus oxychloride (103.5 °C), and discarded. The second fraction was collected when the temperature had stabilised at 103.5 °C. The purity of the $POCl_3$ thus obtained was confirmed by ^{31}P NMR.

Both labeled and unlabeled potassium dihydrogen orthophosphate (KH_2PO_4) were prepared by using a known method [2,23]. In the case of the labeled compound, oxygen-18 labeled water (Novachem) was used in the hydrolysis step. The two reaction steps (hydrolysis followed by neutralisation) are:

$$POCl_3 + 3H_2O \rightarrow H_3PO_4 + 3HCl$$

$$H_3PO_4 + KOH \rightarrow KH_2PO_4 + H_2O$$

Whilst stirring and under positive nitrogen pressure, phosphorus oxychloride was added dropwise, via a syringe, into a septum-sealed single-necked flask containing either nonlabeled ultrapure water, or 94.5% enriched oxygen-18 labeled water. The flask was immersed in an ice bath and, once the violent reaction had subsided, the ice bath was removed and the flask allowed to come slowly to room temperature before heating to 80 °C and maintaining this temperature for a period of two days to ensure complete reaction. During this time, a calcium chloride drying tube was placed over the end of the flask, both to allow HCl gas to escape and to prevent atmospheric water from entering the flask.

After two days, the heat was withdrawn and any remaining HCl removed by rotary evaporation under vacuum at 90 °C for 40 min. The phosphoric acid product was diluted with triply distilled deionised water, and titrated with 1.5 M KOH until a pH of 4.6 was reached (>99.4% phosphate present as $H_2PO_4^-$). This salt solution was again rotary evaporated until a slurry of crystals was visible. The product was recrystallised using a mixed solvent system of water and ethanol. The solid was collected by vacuum filtration using a 0.45 μm membrane (Millipore Teflon, Bradford, MA, USA) and dried at 110 °C for 3 h.

2.2. Electrospray ionisation mass spectrometry (ESI-MS) of orthophosphates

A range of standard KH_2PO_4 solutions was prepared down to 0.1 ppm using both labeled and unlabeled compounds. Sample volumes of 20 μL were injected into the electrospray chamber by way of the autosampler whilst 10 mM ammonium acetate buffer (pH 4.6) was continuously flowing at 0.1 mL min^{-1} into the ion spray chamber. For each analysis, the buffer was freshly prepared immediately prior to analysis. On average, six replicate injections were taken consecutively to obtain a measure of the repeatability of the technique. Triply distilled deionised water was used as a flushing agent between injections.

In a further experiment, the possibility of oxygen exchange with water in the mass spectrometer at elevated temperatures was investigated. Thus, 1000 ppm of unlabeled orthophosphate solution was premixed with a small amount of 94.5% enriched oxygen-18 labeled water and injected into the mass spectrometer.

All ESI-MS experiments were performed using a Perkin-Elmer Sciex API 365 LC/MS/MS system with an Apple Macintosh 8600/200 Power PC. Data were acquired and processed by using LC2 TUNE 1.4 and MULTIVIEW 1.4 software, respectively. Samples were analysed using single ion monitoring and in negative polarity mode with a pause time of 5 ms and a dwell time of 250 ms. The nitrogen nebuliser gas temperature was set at 200 °C. For the variously oxygen-18 labeled orthophosphate species, the mass spectrum from 30 to 500 *m/z* was obtained and analysed.

2.3. ^{31}P nuclear magnetic resonance spectroscopy (^{31}P NMR)

The oxygen isotopic distribution in undiluted orthophosphate was obtained by using ^{31}P NMR spectroscopy on a Bruker 500 MHz instrument operating at 202.455 MHz. A 90° pulse angle of 5.00 μs was used, with an acquisition time of 2.0251 s and a pulse delay of 2.0000 s. Spectra were obtained by using a total of 32 scans. The synthesised compounds were analysed as 10 000 ppm solutions. Commercial potassium dihydrogen orthophosphate (10 000 ppm Ajax Chemicals Analytical Grade) was used as a comparative standard. Standard Bruker packaged Gaussian/Lorentzian deconvolution techniques were used for curve fitting and integration of the NMR peaks. Hence the distribution of the variously oxygen-18 substituted phosphate species was determined.

Comparison was made between the two methods. Simple statistical analyses of the two distributions show differences in the median, standard deviation, skewness, and kurtosis of 0.62%, 2.37%, 6.50%, and 1.24%, respectively. For the ESI- MS method, repeatability on six injections showed the means of the standard deviations of intensities of individual ions was of the order of 3%.

3. Results and discussion

The current work represents a major step in the development of a direct method for determining oxygen isotope ratios as well as quantifying all of the possible oxygen-18 substituted orthophosphate species at the parts per million level. These aspects are discussed in detail.

Possible ions that could be detected by mass spectrometry are given in Table 1 for both unlabeled and labeled experiments. In practice, for the unlabeled orthophosphate experiments, only monoatomic substituted ^{18}O species are observed. For ^{18}O labeled experiments the number of ions present is compli-

Table 1
Exact masses of the major ions predicted in the gas phase from potassium orthophosphate solutions

Ion	*M*	*Z*	*m/z*
$[P^{16}O_3]^-$	78.96	−1	78.96
$[P^{16}O_2{}^{18}O]^-$	80.96	−1	80.96
$[P^{16}O^{18}O_2]^-$	82.97	−1	82.97
$[P^{18}O_3]^-$	84.97	−1	84.97
$[K]^+[HP^{16}O_4]^{2-}$	134.92	−1	134.92
$[H_2P^{16}O_4]^-$	96.97	−1	96.97
$[H_2P^{16}O_3{}^{18}O]^-$	98.97	−1	98.97
$[H_2P^{16}O_2{}^{18}O_2]^-$	100.98	−1	100.98
$[H_2P^{16}O^{18}O_3]^-$	102.98	−1	102.98
$[H_2P^{18}O_4]^-$	104.99	−1	104.99
$[HP^{16}O_4]^{2-}$	95.96	−2	47.98
$[HP^{16}O_3{}^{18}O]^{2-}$	97.97	−2	48.98
$[HP^{16}O_2{}^{18}O_2]^{2-}$	99.97	−2	49.98
$[Hp^{16}O^{18}O_3]^{2-}$	101.97	−2	50.99
$[HP^{18}O_4]^{2-}$	103.98	−2	51.99
$[P^{16}O_4]^{3-}$	94.95	−3	31.65
$[P^{16}O_3{}^{18}O]^{3-}$	96.96	−3	32.32
$[P^{16}O_2{}^{18}O_2]^{3-}$	98.96	−3	32.99
$[P^{16}O^{18}O_3]^{3-}$	100.97	−3	33.66
$[P^{18}O_4]^{3-}$	102.97	−3	34.22

cated because of the possibility of mono, di- or polysubstitution of ^{18}O for ^{16}O.

3.1. Exclusion of equilibrium

For our methodology to be quantitative it is necessary to establish that equilibrium between isotopically different ions is not established. Phosphate mineral $^{18}O/\ ^{16}O$ ratios differ from those of water [24] so that exchange does not occur readily in nature and equilibrium must be slow. Under different conditions (other than electrospray), Kolodny and others have shown that for the reaction involving exchange of oxygen on orthophosphate, attainment of equilibrium at room temperature requires the use of enzymes [12,23]. However this cannot be used as proof that exchange does not occur under the ionisation conditions present in the electrospray mass spectrometer. The likelihood of such exchange occurring is considered in Sec. 3.1.1.

3.1.1. Unlabeled experiments $H_2P^{16}O_4^-$ and $P^{16}O_3^-$

Plots of ion abundance [$m/z = 96.97$, $H_2P^{16}O_4^-$ (y_1) and $m/z = 78.96$, $P^{16}O_3^-$ (y_2)] versus concentration of potassium dihydrogen orthophosphate (x) are shown in Figs. 1 and 2, respectively. The plot in Fig. 1 is not linear but can be fitted to the third order polynomial given by

$$y_1 = 2.4 \times 10^{-2}x^3 - 45.39x^2 + 3574x \quad \text{(correlation coefficient of 0.9945)} \qquad (1)$$

Likewise, the data shown in Fig. 2 for $P^{16}O_3^-$ (y_2) response can be fitted to

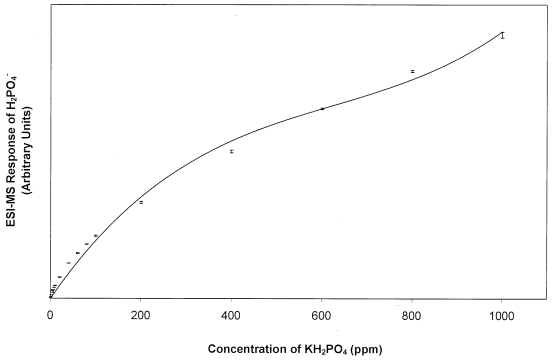

Fig. 1. Calibration curve showing $H_2P^{16}O_4^-$ abundance vs. concentration of synthesised KH_2PO_4 solutions obtained by using mean peak areas of ESI-MS ion chromatograms. Error bars have been calculated as standard errors of the mean of six measurements at each individual concentration. Values on the *y* axis have been omitted for simplicity.

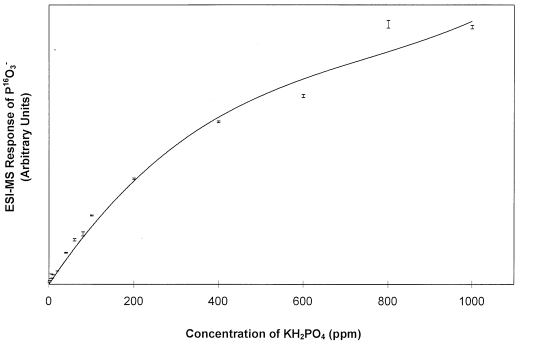

Fig. 2. Calibration curve showing $P^{16}O_3^-$ abundance vs. concentration of synthesised KH_2PO_4 solutions obtained by using mean peak areas of ESI-MS ion chromatograms. Error bars have been calculated as standard errors of the mean of six measurements at each individual concentration. Values on the *y* axis have been omitted for simplicity.

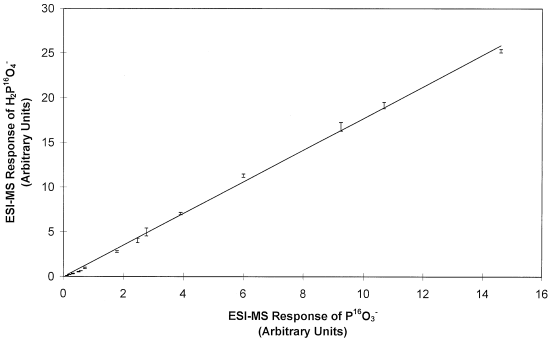

Fig. 3. Linearity of the plot $H_2P^{16}O_4^-$ vs. $P^{16}O_3^-$ abundances by using mean peak areas of ESI-MS ion chromatograms. Error bars have been calculated as standard errors of the mean of six measurements at each individual concentration.

$$y_2 = 2.0 \times 10^{-4}x^3 - 0.3880x^2 + 366.8x$$

(correlation coefficient of 0.9897) (2)

The dihydrogen orthophosphate anion $H_2P^{16}O_4^-$ is the hydrated form of the $P^{16}O_3^-$ anion according to

$$P^{16}O_3^- + H_2{}^{16}O \leftrightharpoons (H_2{}^{16}O)P^{16}O_3^- \quad (3)$$

If equilibrium was established, and water concentration was low, the response may be nonlinear because as additional $(H_2{}^{16}O)P^{16}O_3^-$ is added, the equilibrium would move to oppose the change. In the ionising droplets in the mass spectrometer the concentration of water is not necessarily the same as in solution and water concentration could be small. Such a result, however, should mean that a plot of orthophosphate $[(H_2{}^{16}O)P^{16}O_3^-]$ response versus metaphosphate $[P^{16}O_3^-]$ response should be nonlinear, however such a plot is linear (Fig. 3) strongly suggesting that equilibrium is not established. $\Delta G°$ for the hydration reaction (3) has been calculated as -26.8 kJ mol^{-1} at 1 atm and 298 K [25]. Hence K_1 for this first hydration of the metaphosphate anion can be calculated using $\Delta G° = -RT \log_e K$.

For further hydration $\Delta G° = -20.5$ kJ mol^{-1} according to

$$(H_2{}^{16}O)P^{16}O_3^- + H_2{}^{16}O \leftrightharpoons (H_2{}^{16}O)_2P^{16}O_3^- \quad (4)$$

The third hydration, given by the following reaction has $\Delta G° = -23.0$ kJ mol^{-1}:

$$(H_2{}^{16}O)_2P^{16}O_3^- + H_2{}^{16}O \leftrightharpoons (H_2{}^{16}O)_3P^{16}O_3^- \quad (5)$$

Equilibrium constants for these reactions are also listed in Table 2. Estimates have been made previously of the transition state energy barrier for the first hydration step (41.42 kJ mol^{-1}) [20]. Establishment of equilibrium has a significant energy barrier because it involves transfer of the two protons on water to oxygen on phosphorus and binding the remaining oxygen to the phosphate. The transition state energy barriers for further hydration would be expected to be high and similar in value. However, knowing both $[P^{16}O_3^-]$ and $[(H_2{}^{16}O)P^{16}O_3^-]$, we can calculate the water concentration in the mass spectrometer if equilibrium had been established using the following:

$$[P^{16}O_3^-][H_2{}^{16}O]/[(H_2{}^{16}O)P^{16}O_3^-]$$

$$= 2.03 \times 10^{-5} = 1/K_1$$

The slope of Fig. 3 (1.77) is thus equal to $K_1[H_2{}^{16}O]$, and since K_1 is known, the water concentration in the mass spectrometer at ionisation can be calculated. The value thus obtained is 3.58×10^{-5} mol L^{-1} (i.e. 88.8 Pa; 0.67 Torr; 8.77×10^{-4} atm). These values are somewhat large and suggest that the water concentration is in excess and should not affect the $P^{16}O_3^-$/$(H_2{}^{16}O)P^{16}O_3^-$ response ratio as observed even if equilibrium were established.

Table 2
Equilibrium constants for orthophosphate and related systems

Equilibrium	K	$1/K$
$P^{16}O_3^- + H_2{}^{16}O \rightleftharpoons (H_2{}^{16}O)P^{16}O_3^-$	4.939×10^4	2.03×10^{-5}
$(H_2{}^{16}O)P^{16}O_3^- + H_2{}^{16}O \rightleftharpoons (H_2{}^{16}O)_2P^{16}O_3^-$	3.923×10^3	2.55×10^{-4}
$(H_2{}^{16}O)_2P^{16}O_3^- + H_2{}^{16}O \rightleftharpoons (H_2{}^{16}O)_3P^{16}O_3^-$	1.080×10^4	9.25×10^{-5}

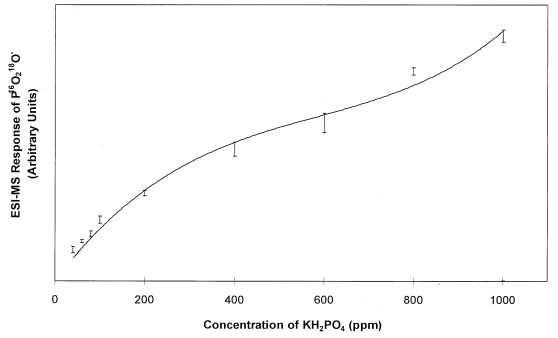

Fig. 4. Calibration curve showing $P^{16}O_2{}^{18}O^-$ natural abundance vs. concentration of commercial KH_2PO_4 solutions obtained by using mean peak areas of ESI-MS ion chromatograms. Error bars have been calculated as standard errors of the mean of six measurements at each individual concentration. Values on the *y* axis have been omitted for simplicity.

3.3.2. Unlabeled experiments: $H_2P^{16}O_3{}^{18}O^-$ and $P^{16}O_2{}^{18}O^-$

A plot of $P^{16}O_2{}^{18}O^-$ response (y_3) against concentration (x) is also nonlinear (Fig. 4) with

$$y_3 = 3.00 \times 10^{-5}x^3 - 0.0471x^2 + 34.60x$$

(correlation coefficient of 0.9886) (6)

Likewise, for $H_2P^{16}O_3{}^{18}O^-$ (y_4), the data (Fig. 5) again follow a third order polynomial function given by

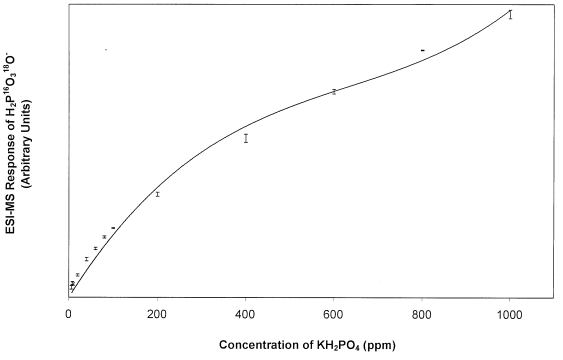

Fig. 5. Calibration curve showing $H_2P^{16}O_3{}^{18}O^-$ natural abundance vs. concentration of commercial KH_2PO_4 solutions obtained by using mean peak areas of ESI-MS ion chromatograms. Error bars have been calculated as standard errors of the mean of six measurements at each individual concentration. Values on the *y* axis have been omitted for simplicity.

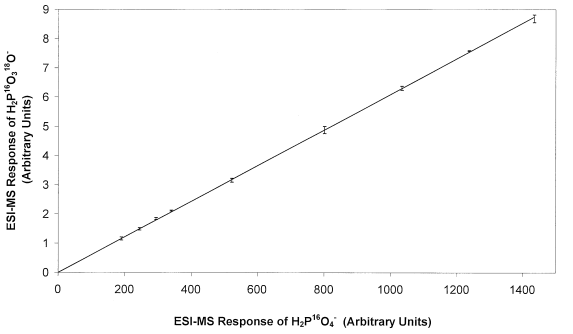

Fig. 6. Linearity of the plot $H_2P^{16}O_3{}^{18}O^-$ vs. $H_2P^{16}O_4^-$ abundances by using mean peak areas of ESI-MS ion chromatograms. Error bars have been calculated as standard errors of the mean of six measurements at each individual concentration.

$$y_4 = 1.00 \times 10^{-4}x^3 - 0.2747x^2 + 218.1x$$

(correlation coefficient of 0.9922) (7)

3.3.3. Unlabeled experiments: $H_2P^{16}O_3{}^{18}O^-$ and $H_2P^{16}O_4^-$

A linear plot of $H_2P^{16}O_3{}^{18}O^-$ versus $H_2P^{16}O_4^-$ response (Fig. 6) may be used to determine the equilibrium constant for the reaction in experiments in which a knowledge of the extent of oxygen exchange is required.

If the exchange:

$$H_2P^{16}O_3{}^{18}O^- + H_2{}^{16}O \leftrightharpoons H_2P^{16}O_4^- + H_2{}^{18}O$$

was occurring in equilibrium, then a plot of $[H_2P^{16}O_3{}^{18}O^-]$ versus $[H_2P^{16}O_4^-]$ (Fig. 6) should yield the equilibrium constant (K) from the slope (slope = $[H_2{}^{18}O]/(K[H_2{}^{16}O])$). The slope of our graph is 0.0061. Given that the $^{18}O/^{16}O$ in standard mean ocean water (SMOW) is 1.993×10^{-3}, tap water is 1.988×10^{-3} [26] and the Vienna standard mean ocean water (V-SMOW) is 2.005×10^{-3} [27], then K is found to be 0.327, 0.325, and 0.329 using the values for SMOW, tap water, and V-SMOW, respectively. All of these values are significantly different from that expected for equilibrium which is close to unity. For example, for the following equilibrium reaction:

$$H_2{}^{18}O + 1/4\ P^{16}O_4^{3-} \leftrightharpoons H_2{}^{16}O + 1/4\ P^{18}O_4^{3-}$$

the equilibrium constants at 0 and 25°C have been reported as 1.0104 and 1.0087, respectively [26].

Finally we were able to confirm that equilibrium is not established experimentally. When 1000 ppm of unlabeled orthophosphate solution was premixed with a small amount of 94.5% enriched oxygen-18 labeled water and injected into a mass spectrometer no enrichment of the phosphate species was observed in the mass spectrometer, confirming that oxygen exchange does not occur under these experimental conditions.

3.2. Explanation of nonlinear behaviour

In the ionising droplets in the mass spectrometer there is competition for the number of charges on the solution droplets [28]. For a linear response there must be a plentiful supply of charges so that all available ions charge. However, at high concentrations this is not so; raising the analyte concentration results in a greater number of ions being evaporated without charge and in this case competition between individual PO_3^- and $(H_2O)PO_3^-$ ions for charge. Thus at elevated concentrations there is increased competition for the number of charges on the solution droplets. This competition for charge gives rise to the observed nonlinearity in the plots.

3.3. Labeled experiments

Mass to charge (m/z) intensities obtained for labeled compounds (y_5, y_6, y_7, y_8, and y_9) as a function of concentration of KH_2PO_4 (x) are shown in Fig. 7. The following equations have been fitted to the five curves, $n =$ 3, 2, 4, 1, and 0, respectively, where n corresponds to the number of ^{18}O substitutions on the phosphate group.

$$y_5 = 6.8 \times 10^{-3}x^3 - 13.08x^2 + 1058x$$
(correlation coefficient of 0.9951) (8)

$$y_6 = 5.0 \times 10^{-3}x^3 - 9.274x^2 + 7233x$$
(correlation coefficient of 0.9956) (9)

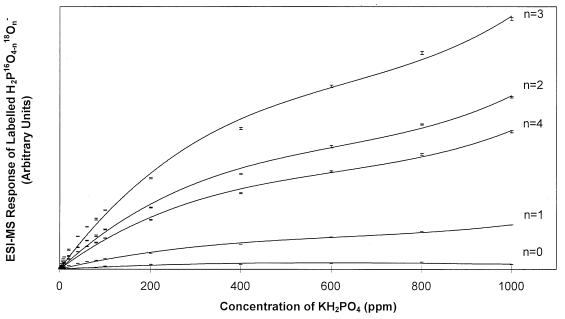

Fig. 7. Calibration curve showing $H_2PO_4^-$ abundance vs. concentration of oxygen-18 labeled KH_2PO_4 solutions showing the various species substituted with three, two, four, one, and zero oxygen 18 isotope labels on the phosphorus atom. Error bars have been calculated as standard errors of the mean of six measurements at each individual concentration. Values on the y axis have been omitted for simplicity.

$$y_7 = 4.1 \times 10^{-3}x^3 - 7.473x^2 + 5780x$$
(correlation coefficient of 0.9962) (10)

$$y_8 = 1.2 \times 10^{-3}x^3 - 2.343x^2 + 1869x$$
(correlation coefficient of 0.9950) (11)

$$y_9 = 2.0 \times 10^{-4}x^3 - 0.5215x^2 + 0.0044x$$
(correlation coefficient of 0.9501) (12)

Comparable data for PO_3^- (y_{10}, y_{11}, and y_{12}) are shown in Fig. 8. The plot is nonlinear because of competition for charge and can be fitted to to the following equations, corresponding to curves of $n =$ 2, 3, and 1, respectively, which in turn, correspond to two, three, and one ^{18}O substituted metaphosphate species:

$$y_{10} = 1.3 \times 10^{-3}x^3 - 2.560x^2 + 2315x$$
(correlation coefficient of 0.9967) (13)

$$y_{11} = 1.1 \times 10^{-3}x^3 - 1.991x^2 + 1743x$$
(correlation coefficient of 0.9970) (14)

$$y_{12} = 6.0 \times 10^{-4}x^3 - 1.149x^2 + 1015x$$
(correlation coefficient of 0.9963) (15)

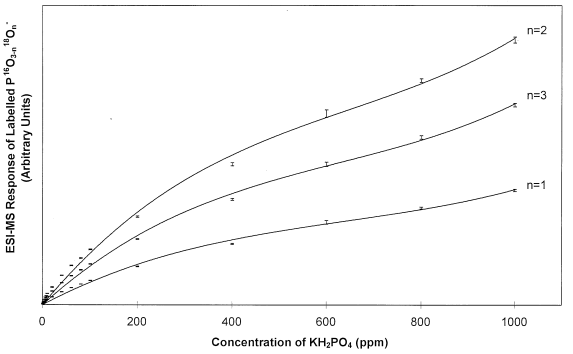

Fig. 8. Calibration curve showing PO_3^- abundance vs. concentration of oxygen-18 labeled KH_2PO_4 solutions showing the various species substituted with two, three, and one oxygen-18 isotope label on the phosphorus atom. Error bars have been calculated as standard errors of the mean of six measurements at each individual concentration. Values on the *y* axis have been omitted for simplicity.

For the dehydration of isotopically labeled orthophosphate there are further considerations to those developed for natural abundance (unlabeled) experiments. There are two possible metaphosphate isotope species that can form from the same orthophosphate isotope species either by the loss of $H_2{}^{16}O$ or $H_2{}^{18}O$. The following equations demonstrate this:

$$H_2P^{16}O_4^- \leftrightharpoons H_2{}^{16}O + P^{16}O_3^- \quad (16)$$

$$H_2P^{16}O_3{}^{18}O \leftrightharpoons H_2{}^{18}O + P^{16}O_3^- \quad (17)$$

$$\leftrightharpoons H_2{}^{16}O + P^{16}O_2{}^{18}O^- \quad (18)$$

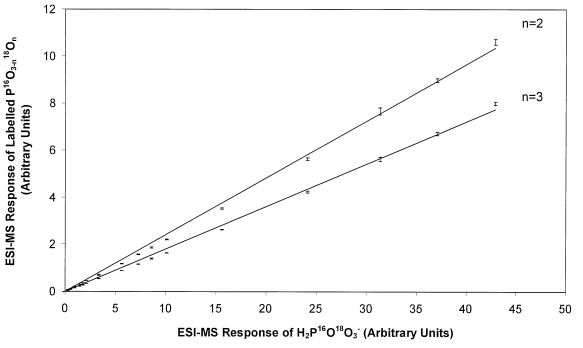

Fig. 10. Linearity of the plots $P^{16}O^{18}O_2^-$ and $P^{18}O_3^-$ vs. $H_2P^{16}O^{18}O_3^-$. Error bars have been calculated as standard errors of the mean of six measurements at each individual concentration.

$$H_2P^{16}O_2{}^{18}O_2^- \leftrightharpoons H_2{}^{18}O + P^{16}O_2{}^{18}O^- \quad (19)$$

$$\leftrightharpoons H_2{}^{16}O + P^{16}O^{18}O_2^- \quad (20)$$

$$H_2P^{16}O^{18}O_3^- \leftrightharpoons H_2{}^{18}O + P^{16}O^{18}O_2^- \quad (21)$$

$$\leftrightharpoons H_2{}^{16}O + P^{18}O_3^- \quad (22)$$

$$H_2P^{18}O_4^- \leftrightharpoons H_2{}^{18}O + P^{18}O_3^- \quad (23)$$

As in the natural abundance experiments, response plots of metaphosphate ions versus orthophosphate ions are linear for the variously labeled species. In this case, plots of $P^{16}O^{18}O_2^-$ and $P^{16}O_2{}^{18}O^-$ versus $H_2P^{16}O_2{}^{18}O_2^-$ (Fig. 9); $P^{16}O^{18}O_2^-$ and $P^{18}O_3^-$ versus $H_2P^{16}O^{18}O_3^-$ (Fig. 10) and $P^{16}O_2{}^{18}O^-$ and $P^{16}O_3^-$ versus $H_2P^{16}O_3{}^{18}O^-$ (Fig. 11) are linear.

In principle, quantitation requires that the sum of

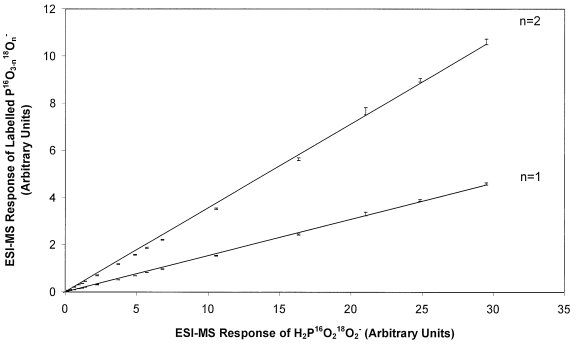

Fig. 9. Linearity of the plots $P^{16}O^{18}O_2^-$ and $P^{16}O_2{}^{18}O^-$ vs. $H_2P^{16}O_2{}^{18}O_2^-$. Error bars have been calculated as standard errors of the mean of six measurements at each individual concentration.

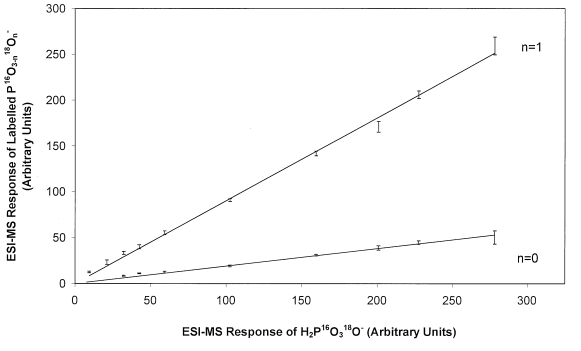

Fig. 11. Linearity of the plots $P^{16}O_2{}^{18}O^-$ and $P^{16}O_3^-$ vs. $H_2P^{16}O_3{}^{18}O^-$. Error bars have been calculated as standard errors of the mean of six measurements at each individual concentration.

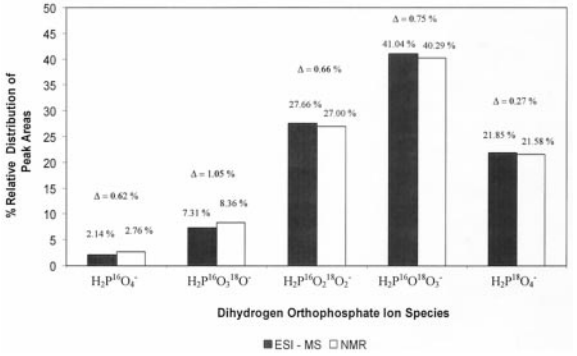

Fig. 12. Graph showing the close correlation between the data obtained by ^{31}P NMR and ESI-MS techniques. Data show percentage relative abundances of the various oxygen-18 labeled species. Differences between the percentage relative abundances obtained by the two techniques have been shown for each labeled species (△).

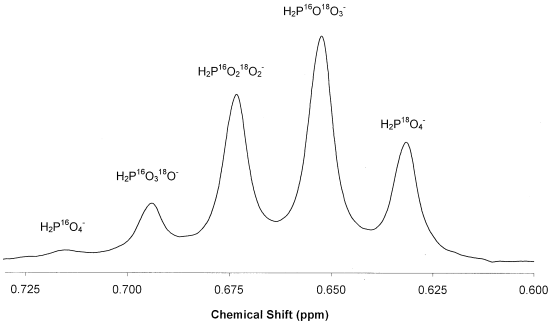

Fig. 13. ^{31}P NMR solution spectrum of isotopically labeled orthophosphate. The variously labeled $H_2PO_4^-$ groups are shown.

the number of moles of both the parent hydrated ion and the dehydrated ion be measured for each species which is isotopically different. Since some of the dehydrated ions can arise for more than one parent, e.g. $P^{18}O_3^-$ in Eqs. 22 and 23, this is difficult. However, if all the reactions proceed to the same extent, that is, any kinetic isotope effects are relatively small compared with the accuracy of measurement, then the sum of the mole fractions for any given species with different isotopic distributions should be representative of the proportions of material present. This is indeed found to be the case. Fig. 12 shows the distribution of labeled phosphates calculated by summing the mole fractions of the $H_2PO_4^-$ ions alone. When these data are compared with those obtained from the NMR spectrum of the undiluted solutions (Fig. 13) good agreement is observed.

We have therefore demonstrated the applicability of the electrospray mass spectrometric method for analysing dihydrogen orthophosphate in solution. Further, the advantage over previous methods is that lengthy analysis requiring precipitation of phosphate over many days is unnecessary. Rapid automated analyses of many samples can be achieved in about an hour. Unlike NMR, parts per million levels can be measured. Thus, only milligram quantities of sample are required for analyses. Moreover, unlike some methods there is no requirement for conversion to a simple gas and indirect evaluation.

Acknowledgements

Jim Keegan is thanked for assistance in running the electrospray ionisation mass spectrometer and Dr. Kamali Kannangara is thanked for assistance with NMR experiments. Rebeca Alvarez is the recipient of a UTS Faculty of Science postgraduate scholarship. Funding from an Australian Research Council SPIRT grant is gratefully acknowledged.

References

[1] H.C. Fricke, J.R. O'Neil, Palaegeogr., Palaeoclimatol., Palaeocol., 126 (1996) 91.
[2] S. Larsen, V. Middleboe, H. Saaby Johansen, Plant Soil 117 (1989) 143.
[3] B. Luz, Y. Kolodny, M. Horowitz, Geochim. Cosmochim. Acta 48 (1984) 1689.
[4] A. Longinelli, Geochim. Cosmochim. Acta 48 (1984) 385.
[5] D. Markel, Y. Kolodny, B. Luz, A. Nishri, Isr. J. Earth Sci. 43 (1994) 165.
[6] A. Longinelli, S. Nuti, Earth Planet. Sci. Lett. 5 (1968) 13.
[7] H. Saaby Johansen, V. Middleboe, S. Larsen, Stable Isotopes in Plant Nutrition, Soil Fertility, and Environmental Studies, International Atomic Energy Agency, Vienna, 1–5 October, 1990, p. 553.
[8] S.M. Savin, J.C.C. Hsieh, Geoderma 82 (1998) 227.
[9] A. Shemesh, Y. Kolodny, B. Luz, Earth Planet. Sci. Lett. 64 (1983) 405.
[10] B. Luz, Y. Kolodny, Earth Planet. Sci. Lett. 75 (1985) 29.
[11] B. Luz, Y. Kolodny, J. Kovach, Earth Planet. Sci. Lett. 69 (1984) 255.

[12] Y. Kolodny, B. Luz, O. Navon, Earth Planet. Sci. Lett. 64 (1983) 398.
[13] P. Iacumin, H. Bocherens, A. Mariotti, A. Longinelli, Earth Planet. Sci. Lett. 142 (1996) 1.
[14] H. Saaby Johansen, Appl. Radiat. Isot. 39 (1988) 1059.
[15] J.R. O'Neil, L.J. Roe, E. Reinhard, R.E. Blake, Isr. J. Earth Sci. 43 (1994) 203.
[16] A.P. Tudge, Geochim. Cosmochim. Acta 18 (1960) 81.
[17] C. Holmden, D.A. Papanastassiou, G.J. Wasserburg, Geochim. Cosmochim. Acta 61 (1997) 2253.
[18] M. Cohn, A. Hu, Proc. Natl Acad. Sci. USA 75 (1978) 200.
[19] R.L. Van Etten, J.M. Risley, Proc. Natl Acad. Sci. USA 75 (1978) 4784.
[20] A.T. Blades, Y. Ho, P. Kebarle, J. Am. Chem. Soc. 118 (1996) 196.
[21] A.T. Blades, Y. Ho, P. Kebarle, J. Phys. Chem. 100 (1996) 2443.
[22] P. Kebarle, Y. Ho, Electrospray Ionization Mass Spectrometry. Fundamentals, Instrumentation, and Applications, Wiley, New York, 1997, p. 3.
[23] H. Saaby Johansen, S. Larsen, V. Middleboe, Appl. Radiat. Isot. 40 (1989) 641.
[24] R.E. Blake, J.R. O'Neil, G.A. Garcia, Geochim. Cosmochim. Acta 61 (1997) 4411.
[25] R.G. Keesee, A.W. Castleman Jr., J. Am. Chem. Soc. 111 (1989) 9015.
[26] K. Rankama, Isotope Geology, Pergamon, London, 1954.
[27] Handbook of Environmental Isotope Geochemistry, The Terrestrial Environment, Vol. 1, P. Fritz, J.C. Fontes (Eds.), Elsevier, Amsterdam, 1980.
[28] G. Wang, R.B. Cole, Electrospray Ionization Mass Spectrometry. Fundamentals, Instrumentation, and Applications, Wiley, New York, 1997, p. 137.